SOCAR

SOCAR Proceedings

Injection & Producing Facilities

journal home page: http://proceedings.socar.az

A NOVEL APPROACH TO LONG-TERM LOAD-CARRYING CAPACITY ASSESSMENT OF CIRCULAR REINFORCED CONCRETE SUPPORT STRUCTURES CONSIDERING HEREDITARY CREEP

M. A. Hajiyev*[1], I. G. Huseynov[2], U. M. Hajiyeva[3], S. R. Bashirzade[1]

[1]*Azerbaijan University of Architecture and Construction, Baku, Azerbaijan*

[2]*Republican Seismic Survey Center, The Azerbaijan National Academy of Sciences, Baku, Azerbaijan*

[3]*«OilGasScientificResearchProject» Institute, SOCAR, Baku, Azerbaijan*

A B S T R A C T

In this study, a multi-step numerical method was suggested for solving the integral constitutive equation for hereditary creep, accounting for the nonlinear characteristics of instantaneous and time-dependent concrete deformations. Numerical verification demonstrates that the method exhibits high computational stability and accuracy, even for relatively large values of time increments in the solution of relaxation problem. By incorporating hereditary creep effects, the long-term loading response of reinforced concrete support structures is practically transferred into a series of incremental short-term static analyses performed at discrete time points. The structural model considers a cantilever circular reinforced concrete member subjected to axial compressive and transverse lateral loads applied at its free end. The proposed computational model enables the determination of the time evolution of the load-carrying capacity and stress–strain state from the initial loading stage to any specific load value. Parametric numerical calculations revealed that low transverse loadings alone caused a considerable loss in the load-carrying capacity. Moreover, through the formulation of a new creep coefficient function from a solution to the relaxation problem, the time-dependent stress–strain behavior and capacity loss were accurately captured using a series of equivalent short-term static analyses. The numerical investigations determined that this creep coefficient function had extremely low sensitivity to load amplitudes, which was predominantly a function of the loading duration. It was quantitatively verified that genetic creep can reduce the load capacity of structural members by a maximum of 30%.

Keywords: concrete; reinforcement; hereditary creep; creep coefficient function; load-carrying capacity.

Date submitted: 05.08.2025 **Date accepted:** 16.11.2025

Introduction

The study proposes advanced methods for analyzing and optimizing geometric configurations while accounting for the physical characteristics of pontoon materials. This methodological approach enhances structural strength and improves the precision of engineering calculations [1]

In the design of supporting systems for stationary offshore platforms, piers are one of the main structural elements, and most of these piers are constructed as reinforced concrete (RC) elements with a circular cross-section. In hydraulic and offshore engineering structures, such elements are commonly used as load-bearing components that operate under complex stress conditions, subject to off-center axial compression and additional horizontal loads. The bearing capacity of such elements is determined not only by the strength of the material but also by their stability, which necessitates additional engineering approaches in the design process [2].

In RC structures, especially during long-term loading, the creep of concrete have a serious impact on the overall behavior and load-bearing capacity of the structure. Therefore, the development of accurate calculation methods that consider the behavior of such elements under both short- and long-term static loads is considered one of the most urgent and fundamental problems in modern structural theory [3]. Several theories have been proposed to model the creep behavior of concrete. However, the most complete and realistic approach among these theories is the nonlinear hereditary creep theory [3]. This theory, which considers the behavior of concrete as a material with deformation memory, can model the interaction of both instantaneous and time-dependent deformations. Studies conducted by well-known researchers show that the nonlinear behavior of concrete in compression should not be limited to long-term loading only but should also be considered for short-term effects [3-5].

Modern international codes and standards, including the Eurocode, recommend the application of a nonlinear deformation model for concrete, even in short-term loading

**E-mail:* hajiyevmukhlis60@gmail.com

http://dx.doi.org/10.5510/OGP20260101159

cases, and present various analytical and empirical dependencies for this purpose [6, 7]. However, in many cases, when developing creep theories, the authors apply nonlinearity only to long-term deformations. However, it is extremely important to consider the nonlinear nature of the instantaneous deformations that occur even during short-term effects. Experimental results show that it is almost impossible to determine the «stress-strain» diagrams with the same accuracy for all levels of short-term loadings using a universal analytical expression. Therefore, some authors have suggested using these experimental diagrams in the form of discrete tables [8]. Although the application of nonlinear «stress-strain» dependencies increases the mathematical complexity of calculations, this approach allows for more accurate modeling of the real behavior of concrete and maximum use of its strength reserve. Thus, a more accurate prediction of the operating mode of the structural elements under loads is ensured. Therefore, the application of nonlinear deformation models is proposed as one of the main requirements for the development of calculation methods in modern construction standards [9, 10]. In recent years, methodologies for considering the creep of concrete gained wide attention in regulatory frameworks [11]. In addition, the important role of the nonlinear deformation model in determining the stress-strain state and load-bearing capacity of reinforced concrete elements under compression has been confirmed by intensive experimental and theoretical studies conducted recently [12]. In this context, the development of computational approaches that consider the nonlinear nature of both instantaneous and hereditary deformation components for both short- and long-term loading conditions is of great scientific and practical importance.

Prediction of creep response of concrete and its effect on structural performance has been studied to a great extent for various types of concrete and in various fields of application. Differences in creep behavior of high-strength and normal-strength concrete are key to structural stability and management of deformation over long periods. Marzouk highlighted the lower creep tendency of high-strength concrete and the importance of considering this feature in the design [13]. Simultaneously, the observation of similar long-term mechanical effects in other structural materials, such as synthetic polyamide ropes used for mooring systems, indicates the universality of deformations formed as a result of long-term loading [14]. This reveals that the creep mechanism is not limited to concrete but also has important significance in various application areas.

In experimental and modeling studies on the creep process in high-performance concrete, models have been developed to determine the primary time-dependent creep behavior [15]. These models form the basis for an accurate assessment of structural durability in long-term analyses of structural durability. Reybrouck et al. experimentally demonstrated that the long-term creep deformation characteristics of prestressed reinforced concrete beams significantly affect their structural bearing capacity [16]. Considerable research effort has also been directed towards modeling the nonlinear response of circular reinforced concrete structures under short- and long-term loading. In this respect, numerical procedures in terms of nonlinear deformation models were proposed by Hajiyeva and applied to some element shapes [17]. Recently, the analysis of RC elements subjected to complex loading conditions has been further improved by the development of nonlinear element models and concrete models of their composition by several authors [18]. The effect of various additives (e.g., industrial waste such as rice husk ash) on the creep mechanism has also been studied, and in some cases, these additives have been shown to reduce the creep rate [19]. In addition, the creep properties of concrete produced with aggregates obtained from recycled concrete waste were analyzed in comparison with existing models [20]. These approaches are related to the development of environmentally sustainable building materials. The flexural behavior and long-term performance of RC structures reinforced with composite materials have also been studied using experimental and theoretical approaches that consider creep effects [21]. In addition, the combined effects of both mechanical and chemical factors play an important role in the design of RC structures used as foundations for corrosion-resistant concrete structures [22]. In this context, creep is an important factor affecting the reduction in bearing capacity over time.

The creep of RC structures is a time-dependent strain phenomenon owing to the rheological characteristics and microstructural formation of the material under prolonged strain over extended periods. The stress intensity and duration, environmental conditions such as temperature and humidity, and microstructural features of the concrete matrix such as porosity, degree of hydration, and interfacial transition zones are all crucial in influencing the magnitude and nature of creep deformation [23]. In addition, the creep response is controlled by technical parameters such as cement type, water-cement ratio, aggregate type, and presence of mineral additives or admixtures, all of which contribute to modifying the viscoelastic and viscoplastic responses over time [23]. Concrete loading age is an important factor; early age loading creates larger creep strains from decreased stiffness and a poorly developed microstructure, whereas later-age loading produces relatively minor deformation. It is noteworthy that controlled preloads, when induced at early maturity levels of concrete, can produce positive effects on the internal structure of the material, that is, hydration products of higher density are developed and porosity is reduced, leading to a lower creep coefficient and improved resistance to long-term deformation [23, 24]. Structurally, creep significantly alters the stress and strain distributions in members, altering both the overall displacements and local force redistributions. In the long run, this can result in excessive long-term deflections, cracking in tension zones, stress relaxation in prestressed and reinforced elements, and potentially hazardous redistribution of internal forces in continuous and redundant structures [24, 25]. In extreme cases, creep deformations can violate both safety and serviceability constraints, particularly in long-span or substantially loaded sections, such as compression members or box girders [25, 26]. To reduce the negative impact of creep, some engineering strategies are used in engineering. These include boosting reinforcement ratios, optimizing cross-sectional geometry, using high-strength or low-shrinkage concrete, and improving construction sequences to reduce early age sustained loads. These processes enhance the long-term stiffness and behavior of the structure, minimizing the potential for lateral movement and rotational distortion during continuous loading [27]. Recent studies have shown that cyclic or repeated loading histories exacerbate creep-induced consequences such loading regi-

mens, where deformation development is accelerated and strain accumulation is greater than that under monotonic loading conditions. This has significant implications for the development of design standards refinement and necessitates the inclusion of cyclic creep in the predictive modeling of new infrastructure that will be exposed to changing operational demands [28]. Experimental programs and theoretical formulations have increasingly focused on improving the predictability and controllability of creep in concrete. In particular, studies on the influence of mechanical load histories and tailored preloading sequences have demonstrated that time-dependent deformation responses can be altered by optimized structural design and optimized load sequencing [29]. These developments offer promising opportunities for integrating creep considerations into future performance-based design frameworks for reinforced concrete structures.

While the reviewed literature does not specifically focus on the influence of creep in pure steel structures [30, 31], several studies highlight the significance of creep effects in composite systems, particularly in concrete-filled steel tube (CFST) arch bridges and other concrete-based structural components [32, 33]. These investigations underscore the critical role of creep in long-term structural reliability. Notably, the variability of creep parameters and the frequent underestimation of creep-induced deformations in current design codes emphasize the need for more accurate prediction models and robust reliability assessment frameworks. Addressing these shortcomings is essential for ensuring the safety and serviceability of structures exposed to sustained loading over extended periods.

Numerical solution of the nonlinear hereditary creep equation of concrete

The creep equation that accounts for the nonlinearity of both short-term and long-term loading of concrete was proposed by one of the leading experts in the field, V. M. Bondarenko [4], and its mathematical expression is given as follows:

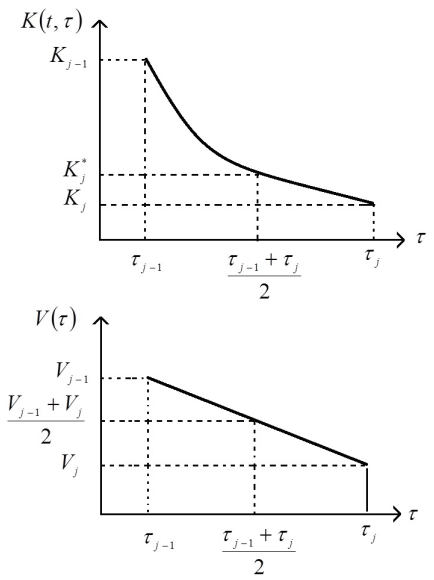

Fig. 1. Schematic representation of the computation of integral limits

$$\varepsilon_b(t) = \frac{1}{E(t)} \cdot U\left(\sigma_b(t)\right) - \int_{t_0}^{t} V\left(\sigma_b(\tau)\right) \cdot K(t, \tau) d\tau \qquad (1)$$

In the proposed formulation, the nonlinear behavior of both the instantaneous (elastic and inelastic) and long-term (viscoelastic and viscous) deformations of concrete is taken into account through approximation functions. These functions, initially introduced by V. M. Bondarenko [3], provide a realistic representation of the actual stress–strain response of concrete under both short-term and sustained loading conditions. By employing such approximations, the model captures the essential features of time-dependent and nonlinear mechanical behavior of concrete, enabling more accurate predictions in structural analysis involving creep.

$$U\left(\sigma_b(t)\right) = \sigma_b(t) \cdot \left[1 + \eta_1 \cdot \left(\frac{\sigma_b(t)}{R_b}\right)^{m_1}\right],$$

$$V\left(\sigma_b(\tau)\right) = \sigma_b(\tau) \cdot \left[1 + \eta_2 \cdot \left(\frac{\sigma_b(\tau)}{R_b}\right)^{m_2}\right] \qquad (2)$$

In addition, considering the time-dependent variation of the elastic modulus of concrete, it was proposed that the kernel of the integral Eq. (1) be expressed in the simplified form $K(t, \tau) = \frac{\partial}{\partial \tau}\left(\frac{1}{E(\tau)} - \frac{1}{E(t)} + C(t, \tau)\right)$ (3), resulting in the modified formulation presented in equation [4].

In this formulation, the function $C(t, \tau)$ represents a basic creep criterion, and its specific mathematical form defines the adopted creep theory for concrete. The integration domain, given by the interval $\tau \in [t_0, t]$, is discretized into n generally unequal subintervals, corresponding to the points $\tau = t_0$, $\tau = \tau_1$, $\tau = \tau_2$, ... , $\tau = \tau_{j-1}$, $\tau = \tau_j$, ... , $\tau = \tau_{n-1}$ and $\tau = \tau_n = t$. Assuming that within each subinterval, the kernel of the integral Eq. (1) can be approximated by a quadratic parabolic function, and the nonlinearity of long-term deformations can be represented by a piecewise linear function, then the integral Eq. (1) can be rewritten as a summation of integrals over these subintervals.

$$\varepsilon_b(\tau_n) = \frac{1}{E(\tau_n)} \cdot U\left(\sigma_b(\tau_n)\right) - \int_{\tau_0}^{\tau_1} V\left(\sigma_b(\tau)\right) \cdot K(t, \tau) d\tau -$$
$$- \int_{\tau_1}^{\tau_2} V\left(\sigma_b(\tau)\right) \cdot K(t, \tau) d\tau - \ldots - \int_{\tau_{n-1}}^{\tau_n} V\left(\sigma_b(\tau)\right) \cdot K(t, \tau) d\tau \qquad (3)$$

It can be demonstrated that each individual integral within the summation can be computed explicitly using the following formulation, as illustrated in figure 1.

$$\int_{\tau_{j-1}}^{\tau_j} K(t, \tau) \cdot V(\tau) d\tau = \frac{\tau_j - \tau_{j-1}}{6} \times$$
$$\times \left[V_{j-1} \cdot \left(K_{j-1} + 2K_j^*\right) + V_j \cdot \left(K_j + 2K_j^*\right)\right] \qquad (4)$$

Where

$$K_j = K(t, \tau_j),\ K_j^* = K\left(t, \frac{\tau_j + \tau_{j-1}}{2}\right),$$

$$V_j = V\left(\sigma_b(\tau_j)\right) = \sigma_b(\tau_j) \cdot \left[1 + \eta_2 \cdot \left(\frac{\sigma_b(\tau_j)}{R_b}\right)^{m_2}\right] \qquad (5)$$

The resulting equation enables the representation of the integral equation describing the nonlinear creep behavior of

concrete in compression as the aforementioned summation of integrals. One of the main advantages of this approach is that it does not require the kernel of the integral equation to be piecewise continuous or smooth. The accuracy of the solution depends primarily on the length of the discretized subintervals introduced during the approximation. Considering this, the general integral equation for an arbitrary number n of subdivisions can be expressed in the following algebraic summation form:

$$\varepsilon_n = \frac{1}{E_n}\cdot U(\sigma_n) - \frac{\tau_n - \tau_{n-1}}{6}\cdot \cdot\left(K_{n,n} + 2\cdot K^*_{n,n}\right)\cdot V(\sigma_n) - W_n \quad (6)$$

The parameter W_n included in this equation accounts for the stress-strain state developed at the preceding time steps and is defined as follows:

$$W_n = -\frac{\tau_1 - \tau_0}{6}\cdot\left[V(\sigma_0)\cdot\left(K_{n,0} + 2\cdot K^*_{n,1}\right) + V(\sigma_1)\cdot\left(K_{n,1} + 2\cdot K^*_{n,1}\right)\right] - \frac{\tau_2 - \tau_1}{6}\times \times\left[V(\sigma_1)\cdot\left(K_{n,1} + 2\cdot K^*_{n,2}\right) + V(\sigma_2)\cdot\left(K_{n,2} + 2\cdot K^*_{n,2}\right)\right] - \\ - .... - \frac{\tau_k - \tau_{k-1}}{6}\cdot\left[V(\sigma_{k-1})\cdot\left(K_{n,k-1} + 2\cdot K^*_{n,k}\right) + V(\sigma_k)\cdot\left(K_{n,k} + 2\cdot K^*_{n,k}\right)\right] - ... - \frac{\tau_{n-1} - \tau_{n-2}}{6}\times \times\left[V(\sigma_{n-2})\cdot\left(K_{n,n-2} + 2\cdot K^*_{n,n-1}\right) + V(\sigma_{n-1})\cdot\left(K_{n,n-1} + 2\cdot K^*_{n,n-1}\right)\right] - \\ - \frac{\tau_n - \tau_{n-1}}{6}\cdot\left(K_{n,n-1} + 2\cdot K^*_{n,n-1}\right)\cdot V(\sigma_{n-1}) \quad (7)$$

Thus, the solution of the integral equation is reduced to addressing the problem of nonlinear short-term effects at discrete time instances.

Assessment of numerical accuracy in solving the relaxation problem

In order to verify the accuracy of the developed numerical algorithm, the solution of a representative relaxation problem is considered. For this purpose, we analyze a simplified case in which the creep coefficient is approximated using the expression $C(t,\tau) = C_0\cdot\frac{e^{\alpha\cdot t} - e^{\alpha\cdot\tau}}{e^{\alpha\cdot t} - 1} + B_0\cdot(e^{-\gamma\cdot\tau} - e^{-\gamma\cdot t})$, representing a basic creep criterion. For heavy concretes $C_0 = 3.8\cdot 10^{-5}$ (MPa)$^{-1}$; $B_0 = 5.7\cdot 10^{-5}$ (MPa)$^{-1}$; $\alpha = 0.3$ (days)$^{-1}$; $\gamma = 0.06$ (days)$^{-1}$, for B20 concrete, the nonlinearity parameters were taken as follows $\eta_1 = 2.0$; $m_1 = 4.7$; $\eta_2 = 2.35$; $m_2 = 4.0$. Accordingly, numerical computations were carried out using the developed program module designed for solving the relaxation problem, and the results of some representative cases are illustrated in figure 2.

As illustrated in figure 2, numerical experiments performed for different discretization step sizes confirmed that the solution maintains sufficient engineering accuracy, even with relatively large steps. For example, in the fifth variant of the previously analyzed case, the fully relaxed stress was determined to be $\sigma_b(\infty) = 7.433$ MPa when a time step of $\Delta t = 0.5$ days was used. It should be noted that for time step sizes of $\Delta t = 5$ days and $\Delta t = 10$ days, the corresponding stress values were obtained as $\sigma_b(\infty) = 7.431$ MPa and $\sigma_b(\infty) = 7.427$ MPa, respectively. This clearly demonstrates the high accuracy of the proposed numerical solution method. Furthermore, the results of the numerical experiments confirmed that, in the case of younger concrete, the time-dependent variation of the elastic modulus has a significant influence on the relaxation process. It was shown that when the loading is applied at $t_0 = 7$ days the initial stress corresponds to 50% and 85% of the compressive strength of concrete, the final relaxed stress increases by $\frac{4.503 - 3.212}{3.212}\cdot 100\% = 40.2\%$ and $\frac{8.683 - 7.431}{7.431}\cdot 100\% = 16.9\%$, respectively, compared to the case with a constant elastic modulus. This indicates a significant influence of the time-dependent variation of the elastic modulus on the relaxation behavior in younger concretes. Additionally, it was demonstrated that for sufficiently mature concretes, the influence of elastic modulus variation on the final relaxed stress becomes negligible when is loading time step sizes $t_0 = 60$ days. In such cases, the final relaxed stress obtained under the assumption of a constant elastic modulus is slightly higher than the value obtained considering its variation. Furthermore, calculations corresponding to the loading time confirmed that when the initial stress level equals 50 and 85% of the compressive strength, the relaxed stress is 8.4 and 4.25% lower, respectively, in the case of a time-dependent elastic modulus compared to the constant modulus case.

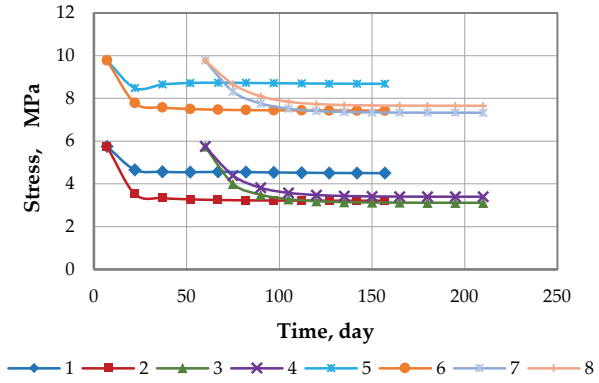

1 - $\sigma_b = 0.5R_b$; $t_0 = 7$ days, when the elastic modulus is variable
2 - $\sigma_b = 0.5R_b$; $t_0 = 7$ days, when the elastic modulus is constant
3 - $\sigma_b = 0.5R_b$; $t_0 = 60$ days, when the elastic modulus is variable
4 - $\sigma_b = 0.5R_b$; $t_0 = 60$ days, when the elastic modulus is constant
5 - $\sigma_b = 0.85R_b$; $t_0 = 7$ day, when the elastic modulus is variable
6 - $\sigma_b = 0.85R_b$; $t_0 = 7$ days, when the elastic modulus is constant
7 - $\sigma_b = 0.85R_b$; $t_0 = 60$ days, when the elastic modulus is variable
8 - $\sigma_b = 0.85R_b$; $t_0 = 60$ days, when the elastic modulus is constant

Fig. 2. Stress relaxation curve

Study on the stress-strain behavior and load capacity of compressed structural members

To determine the stress-strain state and load-carrying capacity of circular cross-section reinforced concrete support structures subjected to combined compression and bending, an appropriate numerical methodology is developed. Based on the proposed methodology, numerical experiments are conducted to investigate the influence of nonlinear hereditary creep of concrete on the stress-strain behavior of the structural elements.

Assuming the distribution of compressive stresses in concrete across the section follows the relationship proposed by

V. M. Bondarenko [4], and taking the origin of the coordinate system at the center of the cross-section, the distribution of stresses across the section can be expressed as follows:

$$\sigma_{bz} = \sigma_b \cdot \left(\frac{z + x - R}{x} \right)^{n_\sigma} \tag{8}$$

In this expression, the compressive stress distribution in concrete is described using a stress block shape parameter, denoted by $n_\sigma = 1 - (1 - f_0) \cdot \left(\frac{\sigma_b}{R_b} \right)^{m_\sigma}$, as proposed in [4]. Based on experimental studies, the parameter $m_\sigma = \frac{2m_1}{3}$, and for conventional heavyweight concrete, the value f=0.11 is recommended [4]. Accordingly, the internal normal force and bending moment resulting from the stress distribution over the section are obtained as follows:

$$N_b(\sigma_b, x) = 2\sigma_b \cdot \int_q^R \left(\frac{z + x - R}{x} \right)^{n_\sigma} \cdot \sqrt{R^2 - z^2}\, dz; \tag{9}$$

$$M_b(\sigma_b, x) = 2\sigma_b \cdot \int_q^R \left(\frac{z + x - R}{x} \right)^{n_\sigma} \cdot z \cdot \sqrt{R^2 - z^2}\, dz \tag{10}$$

Here, the lower limit of the integral is defined as $q = \begin{cases} -R, & when \;\; x \geq 2R \\ R - x, & when \;\; 0 < x < 2R \end{cases}$, depending on the position of the neutral axis. Similarly, assuming that the reinforcing bars deform according to a bilinear stress-strain diagram, the stress in an arbitrary j-th reinforcement bar (fig. 3) can be expressed as follows:

$$\sigma_{s,j}(\varepsilon_b, x) = \begin{cases} E_{s,j} \cdot \frac{\varepsilon_b}{x} \cdot (R_{s,j} \cdot \sin\varphi_{s,j} + x - R); \\ \quad if \;\; \left| \frac{\varepsilon_b}{x} \cdot (R_{s,j} \cdot \sin\varphi_{s,j} + x - R) \right| \leq \varepsilon_{s,ax} \\ R_{s,j} \cdot sign\left(\frac{\varepsilon_b}{x} \cdot (R_{s,j} \cdot \sin\varphi_{s,j} + x - R) \right); \\ \quad if \;\; \left| \frac{\varepsilon_b}{x} \cdot (R_{s,j} \cdot \sin\varphi_{s,j} + x - R) \right| \leq \varepsilon_{s,ax} \end{cases} \tag{11}$$

Accordingly, the internal normal force and bending moment arising in the reinforcement bars are determined using the following expressions:

$$N_s(\varepsilon_b, x) = \sum_{j=1}^{K_s} \sigma_{s,j}(\varepsilon_b, x) \cdot A_{s,j};$$

$$M_s(\varepsilon_b, x) = \sum_{j=1}^{K_s} \sigma_{s,j}(\varepsilon_b, x) \cdot A_{s,j} \cdot R_{s,j} \cdot \sin\varphi_{s,j} \tag{12}$$

Based on the obtained expressions, the equilibrium equations for the most highly stressed section of the support structure are formulated as follows:

$$N_b(\sigma_b, x) + N_s(\varepsilon_b, x) = P \tag{13}$$

$$M_b(\sigma_b, x) + M_s(\varepsilon_b, x) = P(e + f) + Q \cdot l \tag{14}$$

In this equation, P denotes the compressive axial force, and e represents the eccentricity of the compressive force as shown in figure 4. If the deformed axis of the support structure is approximated by the function

$$y(x) = f \cdot \left(1 - \cos\frac{\pi \cdot x}{2l} \right) \tag{15}$$

[1, 12], then the curvature at this section can be expressed as

$$\chi = f \cdot \frac{\pi^2}{4l^2} \tag{16}$$

On the other hand, according to the computational scheme, the curvature at this section is given by $\chi = \frac{\varepsilon_b}{x}$. From these two equations, the maximum deflection of the support at the most stressed section can be expressed as the concrete strain at the compressed face and the height of the compressed zone of the section, given by

$$f = \rho_0 \cdot \frac{\varepsilon_b}{x} \tag{17}$$

where ρ_0 is a parameter defined as in

$$\rho_0 = \frac{4l^2}{\pi^2} \tag{18}$$

The obtained Eq.s (6), (13), and (14), when considered with respect to the parameters ε_b, σ_b and x constitute a system of nonlinear governing equations for the problem under study.

Study on the structural behavior of reinforced concrete members under short-term loading

It should be noted that the investigation of the stress-strain behaviors of the support structure under short-term

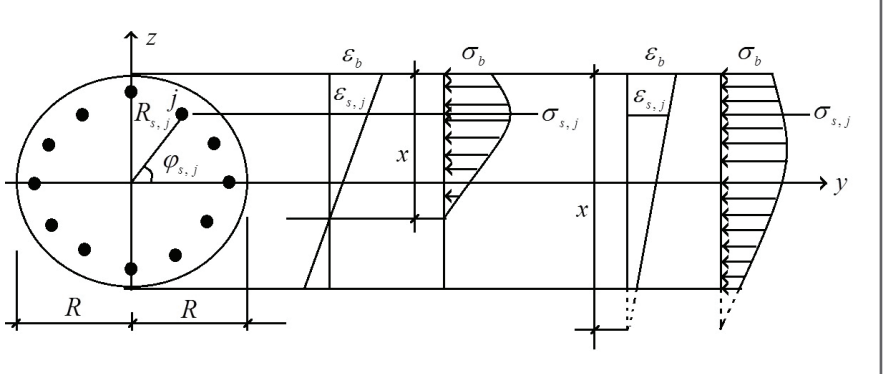

Fig. 3. Cross-section model

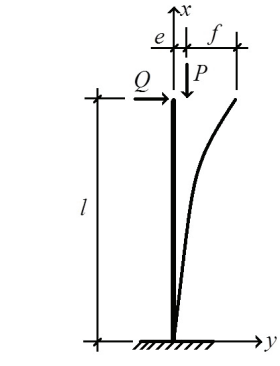

Fig. 4. Computational scheme of the cantilever support element

static loading holds particular significance. Therefore, this issue is examined separately. In this case, the system of governing equations again consists of Eq.s (13) and (14), supplemented by Eq. (6) at the initial condition, expressed as

$$\varepsilon_b = \frac{1}{E_b} \cdot U(\sigma_b) \qquad (19)$$

To construct the numerical solution of this system, the numerical method proposed by the first author is employed [12]. The essence of this methodology lies in the fact that since the variation range of the compressive stress in the concrete at the compressed face of the section is known as a priori, the value of this parameter is assumed accordingly.

At this stage, the parameters ε_b and n_σ become known numerical values. In the subsequent calculations. It is assumed that $Q=\nu \cdot P$, the horizontal force acting at the free end of the support is expressed as a certain proportion of the axial compressive force. By eliminating the force parameter from Eq.s (13) and (14), we obtain a nonlinear algebraic equation with a single unknown, formulated with respect to the height of the compressed zone of the cross-section, denoted by the parameter x:

$$\Psi(x) = M_b(\sigma_b, x) + M_s(\varepsilon_b, x) - \\ -\left(N_b(\sigma_b, x) + N_s(\varepsilon_b, x)\right) \cdot \left(e + \rho_0 \cdot \frac{\varepsilon_b}{x} + \nu \cdot l\right) = 0 \qquad (20)$$

This nonlinear equation can be solved using any standard numerical method, such as the bisection method, to determine the parameter x with the desired level of accuracy. As a result, the corresponding values of σ_b, ε_b, n_σ, x, f determined for the assumed compressive stress level. Subsequently, the corresponding axial compressive force is evaluated from Eq. (13), allowing the construction of the «load–displacement» curve, which plays a critical role in determining the load-carrying capacity of compressed members.

A computational module implementing this solution algorithm has been developed and utilized for various numerical experiments. In these calculations, the concrete grade was taken as B20, the reinforcement type as A400, and the column height was assumed to be 10 meters with a cross-sectional radius of R=0.2 m. The cross-section was assumed to be reinforced with 12 evenly distributed longitudinal bars with a diameter of 28 mm.

As a result of the analyses, the displacement curve is presented in figure 5, clearly demonstrating the significant influence of horizontal forces on the load-carrying capacity of compressed structural members. Notably, when no horizontal force is applied, the diagram exhibits a descending branch, indicating post-peak softening behavior. As the magnitude of the horizontal force increases, both the load-bearing capacity and stiffness of the system decrease drastically. For instance, when the ratio of the horizontal to axial force increases from 0 to 0.1 and 0.5, the load-carrying capacity of the column decreases by factors of approximately 4.2 and 15.8, respectively. This effect is attributed to the substantial moment generated by the horizontal force due to its significant lever arm in the structural configuration.

Study on the structural behavior of reinforced concrete members under long-term loading

Now, the solution of the problem under long-term loading conditions is described as follows: For an arbitrary value

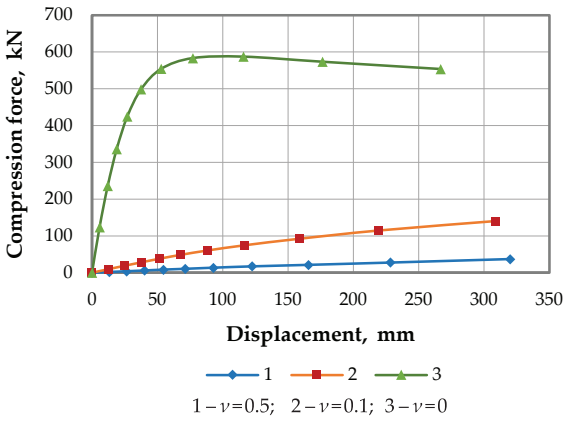

Fig. 5. Load -dispacement curve of RC member

of n, the governing system of equations for the problem can be written as follows:

$$\begin{cases} \varepsilon_{bn} = \dfrac{1}{E_n} \cdot U(\sigma_{bn}) - \dfrac{\tau_n - \tau_{n-1}}{6} \cdot \left(K_{n,n} + 2 \cdot K^*_{n,n}\right) \cdot V(\sigma_{bn}) - W_n \\ N_b(\sigma_{bn}, x_n) + N_s(\varepsilon_{bn}, x_n) = P \\ M_b(\sigma_{bn}, x_n) + M_s(\varepsilon_{bn}, x_n) = P \cdot \left(e + \rho_* \cdot \dfrac{\varepsilon_{bn}}{x_n} + \nu \cdot l\right) \end{cases} \qquad (21)$$

As mentioned above, for the introduced n-th time step, the parameter W_n is calculated based on Eq. (7). Since it is not possible to derive an analytical solution for the resulting system, a numerical solution approach is employed. The essence of the numerical method lies in the fact that the variation range of the compressive stress in the concrete is known in advance. Therefore, the value of compressive stress is assumed to start from a very small value ($\sigma_{bn}=\sigma_{bna}$). Corresponding to this assumed value of stress, the strain is computed using the first equation of system (21). Then, by eliminating the compressive force parameter from the second and third equations of system (21), the following relation is obtained between the parameters ε_{bn} and σ_{bn}:

$$\Omega(x_n) = M_b(\sigma_{bn}, x_n) + M_s(\varepsilon_{bn}, x_n) - \\ -\left(N_b(\sigma_{bn}, x_n) + N_s(\varepsilon_{bn}, x_n)\right) \cdot \left(e + \rho_* \cdot \frac{\varepsilon_{bn}}{x_n} + \nu \cdot l\right) = 0 \qquad (22)$$

This equation, at known values of the parameters ε_{bn} and σ_{bn} allows the parameter x_n to be determined numerically with any desired level of accuracy as the root of a nonlinear equation with a single unknown.

Subsequently, based on the second equation of the system, the compressive force $P_a = N_b(\sigma_{bna}, x_n) + N_s(\varepsilon_{bn}, x_n) - P$ corresponding to the assumed stress value is calculated. In the next step, the stress value is incremented by a predefined step, and the calculations are repeated to obtain a new value of compressive force $P_b = N_b(\sigma_{bnb}, x_n) + N_s(\varepsilon_{bn}, x_n) - P$. If the signs of P_a and P_b are the same, then the assumed values $\sigma_{bna}=\sigma_{bnb}$ and $P_a=P_b$ are updated, and the process continues until the signs of and become opposite. In this way, the interval $\sigma_{bn} \in [\sigma_{bna}, \sigma_{bnb}]$ containing the root of the equation is identified. The root within this interval is then determined with the required accuracy using the bisection method. Once the stress value for the accepted value of n is found, other parameters characterizing the stress–strain state can be easily calculated using the previously defined relationships By repeating the procedure for each value of n, the parameters

that define the stress–strain behavior at various time instances are determined based on the described solution algorithm. Thus, when nonlinear creep of concrete is considered, the long-term problem is reduced to a series of short-term nonlinear static analyses using transformed stress–strain diagrams corresponding to specific time steps. Although the presented solution is numerical, it provides a precise solution to the problem under the assumed hypotheses. As demonstrated earlier, the method allows for the solution to be constructed with any required level of engineering accuracy.

Engineering methodology for considering creep effects

In this methodology, creep behavior of concrete is approximated through the use of a creep coefficient. In this approach, the elastic modulus in the concrete's short-term static load «stress-strain» relationship is modified to account for creep by incorporating the creep coefficient into the expression $\frac{E_{bt}}{1+\varphi_{t,t_0}}$. As a result, instead of the integral equation of the nonlinear hereditary creep theory of concrete, the following equality can be written:

$$\varepsilon_{bt}=\left(1+\varphi_{t,t_0}\right)\cdot\frac{\sigma_{bt}}{E_{bt}}\cdot\left[1+\eta_1\cdot\left(\frac{\sigma_{bt}}{R_b}\right)^{m_1}\right] \tag{23}$$

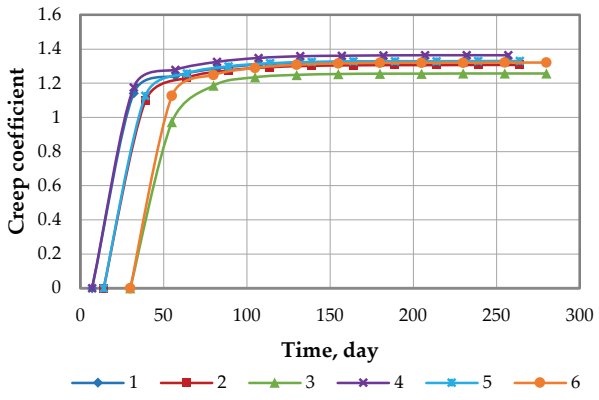

Fig. 6. Variation of the creep coefficient for B40 class concrete

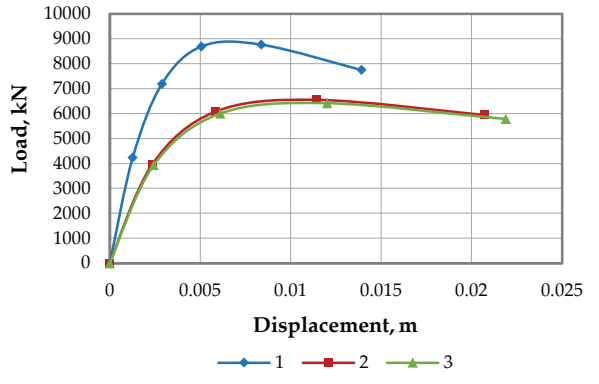

1 – At initial time t_0=14 days under short-term loading without considering creep;
2 – At time t=30 days considering creep;
3 – At time t=264 days considering creep

Fig. 7. Load-displacement curves considering concrete creep

It is proposed to determine the value of the creep coefficient φ_{t,t_0} included in this equation from the solution of the relaxation problem. Thus, from Eq. (23), the following expression for the creep coefficient can be written:

$$\varphi_{t,t_0}=\frac{E_{bt}\cdot\varepsilon_{bt}}{\sigma_{bt}\cdot\left[1+\eta_1\cdot\left(\frac{\sigma_{bt}}{R_b}\right)^{m_1}\right]}-1 \tag{24}$$

In this case, for an arbitrary time instant t, the governing system of equations can be written as follows:

$$\begin{cases}\varepsilon_{bt}=\left(1+\varphi_{t,t_0}\right)\cdot\dfrac{\sigma_{bt}}{E_{bt}}\cdot\left[1+\eta_1\cdot\left(\dfrac{\sigma_{bt}}{R_b}\right)^{m_1}\right]\\ N_{bt}\left(\sigma_{bt},x_t\right)+N_{st}\left(\varepsilon_{bt},x_t\right)=P\\ M_{bt}\left(\sigma_{bt},x_t\right)+M_{st}\left(\varepsilon_{bt},x_t\right)=P\cdot\left(e+\rho_0\cdot\dfrac{\varepsilon_{bt}}{x_t}+\nu\cdot l\right)\end{cases} \tag{25}$$

For various time instances, this system is solved to determine the key parameters characterizing the stress-strain state, namely σ_{bt}, ε_{bt}, and x_t. Subsequently, other parameters can be easily calculated using the formulas presented above. The solution algorithm for system (25) is performed in the same manner as described in the second section for short-term loadings. The methodology for determining the creep coefficient is illustrated through numerical examples.

The relaxation problem is solved for concrete of class B40 using the methodology described in the previous sections. For this concrete class R_b=22 MPa, the time-dependent variation of the elastic modulus is given by $E_{bt}(\tau)=E_{b0}\cdot(1-\alpha_E\cdot e^{-\beta_E\cdot\tau})$, E_{b0}=39920 MPa, α_E=0.573 and β_E=0.063 (days)$^{-1}$. η_1=1.0; m_1=3.8; η_2=1.22; m_2=4.0. For this concrete, when the initial stress corresponds to 50% and 85% of the strength limit, the time-dependent variation of the creep coefficient for different loading times is presented in figure 6. The conducted calculations have shown that the loading time and loading level have a very weak influence on the stabilized value of the creep criterion. This indicates that, in engineering problem-solving, the proposed relation (23) can be effectively applied to directly determine the stabilized stress-strain state. In figure 6, the first three legends (1, 2 and 3) correspond to the loading level where the initial stress is 50% of the concrete strength limit, with the loading times corresponding to moments t_0=7 days, t_0=14 days and t_0=30 days, respectively. Similarly, the next three legends (4, 5 and 6) represent the case where the initial stress corresponds to 85% of the concrete compressive strength limit. The loading times are assumed to be the same across all legends.

Now, based on the previously proposed solution methodology, a column with a cross-sectional radius of r and a height of h, reinforced with uniformly distributed 28 mm diameter bars, made of B40-class concrete and A400-class steel, is considered. The column is subjected to axial compression with a small eccentricity e=0.01 m.It should be noted that once the numerical solution algorithm for system (25) which allows solving with any desired accuracy — is implemented in a dedicated program module, conducting numerical experiments becomes straightforward. Such a program module was developed and applied to carry out numerical experiments. Some of the results from these numerical experiments are presented in figure 7, illustrating the load-displacement curves, which are crucial for deter-

mining the load-carrying capacity of the column.

Based on figure 7, it should be noted that the load-bearing capacities of the element at the considered time instances were determined as $P_{ult(14)}$=8762.7 kN, $P_{ult(39)}$=6548.6 kN and $P_{ult(264)}$=6412.3 kN, respectively. This indicates that due to the creep behavior of concrete, the load-bearing capacity of the element under concentrically compressed conditions decreased by 26.8%. At the points of capacity loss in the examined cases, the maximum deflections of the element were $f_{ult(14)}$=8.37 mm, $f_{ult(39)}$=11.44 mm and $f_{ult(264)}$=12.03 mm respectively. This clearly demonstrates that for structural elements made from materials exhibiting creep properties, the load-bearing capacity of compressed members must be assessed with creep effects duly considered.

Conclusions

In this study, a comprehensive investigation was conducted on the nonlinear hereditary creep behavior of concrete in compressed reinforced concrete elements, considering both the short-term and long-term loading effects. Several critical findings and methodological contributions have been achieved.

- An efficient numerical solution method is proposed for the integral equation of hereditary creep in concrete, accounting for the nonlinearity of both short- and long-term loading effects.
- It has been demonstrated that the proposed solution methodology for solving relaxation problems yields results with engineering-level accuracy, even when relatively large solution time intervals are used.
- It has been shown that the time-dependent increase in the modulus of elasticity of concrete has a more significant impact on the final stabilized relaxation stress in younger concrete compared to older concrete.
- Under short-term static loading, the effect of horizontal forces acting on the column significantly influences the load-bearing capacity of structural elements and should be considered in calculations.
- An effective numerical methodology was developed to determine the stress–strain state and load-carrying capacity by considering concrete creep. The proposed solution approach transforms the long-term loading problem into a sequence of equivalent short-term loading problems at different time stages.
- A simplified engineering methodology for accounting for creep was proposed by introducing a creep coefficient function. It has been demonstrated that creep in compressed concrete elements leads to a reduction in the load-bearing capacity.

References

1. Aslanov, L. F., Aslanli, U. L., Aslanov, F. L. (2025). New calculation method for the pontoon element of offshore fixed platforms for oil and gas production. *Nafta-Gaz*, 3, 188–198.

2. Hajiyev, M. A., Guseynov, I. G., Gadjiyeva, U. M. (2023). Stress-strain state and load ability of compressed pipe-concrete elements. *SOCAR Proceedings*, 1, 21–26.

3. Beglov, A. D., Sanzharovsky, R. S. (2011). Eurocode and nonlinear theory of reinforced concrete. St. Petersburg.

4. Bondarenko, V. M., Bondarenko, S. V. (1982). Engineering methods of the nonlinear theory of reinforced concrete. *Moscow: Stroyizdat*.

5. Golyshev, A. B., Kolchunov, V. I., Yakovenko, I. A. (2015). Theory and design of reinforced concrete structures considering long-term processes. *Kyiv: Talcom.*

6. Kolmogorov, A. G., Plevkov, V. S. (2014). Design of reinforced concrete structures according to russian and foreign standards. *Moscow: ASV.*

7. Babich, V. I., Kochkarov, D. V. (2014). Design of reinforced concrete structural elements using the deformation method. *Concrete and Reinforced Concrete*, 2, 12–16.

8. Hajiyeva, U. M. (2021). Investigation of the load-bearing capacity of compressed reinforced concrete elements based on tabular diagrams. *Scientific Works, AzUAC*, 2, 67–76.

9. SP 63.13330.2012. (2013). Code of practice. Concrete and reinforced concrete structures. General provisions. Updated edition of SNiP 52-01-2003. *Moscow: Consultant Plus.*

10. Kodysh, E. M., Nikitin, I. K., Trekin, N. R. (2010). Design of reinforced concrete structures made of heavy concrete for strength, crack resistance, and deformations. *Moscow: ASV.*

11. Sanzharovsky, R. S., Manchenko, M. M. (2017). Nonlinear theory of creep of concrete and reinforced concrete and modern standards. *Structural Mechanics of Engineering Constructions and Buildings*, 1, 23–35.

12. Hajiyev, M., Damirov, M. (2023). Stress-strain state and bearing capacity of compressed reinforced concrete elements of annular section. *Architectural Studies*, 2(9), 35–46.

13. Marzouk, H. (1991). Creep of high–strength concrete and normal–strength concrete. *Magazine of Concrete Research*, 43(155), 121–126.

14. Civier, L., Chevillotte, Y., Bles, G., et al. (2022). Short and long term creep behaviour of polyamide ropes for mooring applications. *Ocean Engineering*, 259, 111800.

15. Le Roy, R., Le Maou, F., Torrenti, J. M. (2017). Long term basic creep behavior of high performance concrete: data and modelling. *Materials and Structures*, 50(1), 85.

16. Reybrouck, N., Van Mullem, T., Taerwe, L., Caspeele, R. (2020). Influence of long-term creep on prestressed concrete beams in relation to deformations and structural resistance: Experiments and modeling. *Structural Concrete*, 21(4), 1458–1474.

17. Gadzhieva, U. M. K. (2021). Design of compressed reinforced concrete elements with circular cross-section using the nonlinear deformation model. *Expert: Theory and Practice*, 5(14), 13–20.

18. Bashirzade, S. R., Hajiyev, M. A., Lipin, A. A., et al. (2025). Comprehensive study on nonlinear analysis of RC members under combined loads using advanced element and concrete models. *International Journal on Technical and Physical Problems of Engineering (IJTPE),* 17(1), 392–402.

19. He, Z. H., Li, L. Y., Du, S. G. (2017). Creep analysis of concrete containing rice husk ash. *Cement and Concrete Composites*, 80, 190–199.

20. Silva, R. V., De Brito, J., Dhir, R. K. (2015). Comparative analysis of existing prediction models on the creep behaviour of recycled aggregate concrete. *Engineering Structures*, 100, 31–42.

21. Hajiyev, M. A., Aeinehchi, S., Bashirzade, S. R., et al. (2024). Study on the flexural performance of reinforced concrete structures strengthened with composites. *Scientific and Technical Journal on Engineering Mechanics*, 8(2), 16.

22. Garibov, R. B., Bashirzade, S. R., Gadzhieva, U. M., Rzaeva, Ch. G. (2018). Design of corrosion-resistant foundations. In: *Durability of building materials, products, and structures.*

23. Chiorino, M. A. (2005). A rational approach to the analysis of structural effects due to creep. *ACI Special Publication*, 227, 107–142.

24. Daou, H., Raphael, W., Geara, F. (2022). Evaluation of factors affecting long-term creep of concrete using machine learning regression models. In: Bridge safety, maintenance, management, life-cycle, resilience and sustainability. *CRC Press.*

25. Guo-hui, C. A. O. (2009). Long-term behavior analysis of concrete continuous box girder. *Engineering Mechanics*, 26(3), 155–160.

26. Tošić, N. D., Marinković, S. B., Ignjatović, I. S., et al. (2017, August). Experimental setup for measuring long-term behavior of green reinforced concrete beams. In: High tech concrete: Where technology and engineering meet. Proceedings of the 2017 FIB Symposium, Maastricht, The Netherlands, June 12–14. *Cham: Springer International Publishing.*

27. Reybrouck, N., Criel, P., Caspeele, R., Taerwe, L. (2015). Modelling of long-term loading tests on reinforced concrete beams. *Concreep* 10, 745–753.

28. Zivaljevic, S., Tomanovic, Z. (2022). Loading history effect on time-dependent deformations after unloading – reversible creep of soft rock (marl). *Mechanics of Time-Dependent Materials*, 26(3), 499–530.

29. Kammouna, Z., Briffaut, M., Malecot, Y. (2019). Experimental study of the creep effect on the mechanical properties of concrete. *Advances in Civil Engineering*, 1, 5907923.

30. Lipin, A., Bashirzade, S., Hajiyev, M., Garibov, R. (2025). Impact of design and construction errors on the structural reliability of steel industrial buildings. *Reliability: Theory & Applications*, 20(1(82)), 903-917.

31. Sýkora, M., Nadolski, V. (2022). Reliability approaches affecting sustainability of existing steel structures. *Acta Polytechnica CTU Proceedings*, 38, 104-109.

32. Chen, Z., Gao, F., Hu, J., et al. (2023). Creep and shrinkage monitoring and modelling of CFST columns in a super high-rise under-construction building. *Journal of Building Engineering*, 76, 107282.

33. Terry, P. J., Bradford, M. A., Gilbert, R. I. (2021). Creep and shrinkage in concrete-filled steel tubes. In: *Tubular structures. Routledge.*